Simulation of HCCI combustion in air-cooled off-road engines fuelled with diesel and biodiesel.

José Antonio Vélez Godiño, Francisco José Jiménez-Espadafor Aguilar, Miguel Torres García.

Thermal Power Group, Department of Energy Engineering, University of Seville.

Escuela Técnica Superior de Ingeniería de Sevilla, Camino de los Descubrimientos, s/n, 41092, Seville, Spain.

1. Abstract

The present work describes the elaboration of a predictive tool consisting on a phenomenological multi-zone model, applicable to the simulation of HCCI combustion of both diesel and biodiesel fuels. The mentioned predictive tool is created with the aim to be applied in the future to perform engine characterization during both pre-design and post-design stages. The methodology applied to obtain the proposed predictive model is based on the generation of an analytical mechanism that, given a set of regression variables representing the engine operative conditions, provides the user with the optimal figures for the scaling coefficients needed to particularize both the ignition delay and the heat release rate functional laws, which rule the combustion development in the proposed multi-zone model for HCCI engines. The validation of the proposed predictive multi-zone model consists on the comparison between chamber pressure curve derived from the simulations and experimental data based on a DEUTZ FL1 906 unit modified in order to allow HCCI combustion operation mode using diesel EN590 and rapeseed biodiesel. Finally, evidences of the capabilities of the proposed model to be used as a predictive tool applicable to the analysis of off-road engines under HCCI conditions are provided, consisting in the characterization and optimization of the operational maps related to both Brake Specific Fuel Consumption and NOx emissions.

2. Introduction

According to the International Energy Agency (IEA) [1], fuel consumption will increase steadily over the period to 2040, to help meet a one-third rise in global energy demand. However, the same source states that global emissions of particulate matter (PM), sulphur dioxide (SO2) and nitrogen oxides (NOx) are

projected to fall over the same period, as a consequence of energy and climate regulations. Table 1 shows the variations (related to 2016), by some regions, derived from the IEA projections by 2040 regarding SO2, NOx and PM.

Region	SO2	NOx	PM
United States	-50%	-50%	-33%
European Union	-47%	-55%	-20%
China	-30%	-30%	-40%
India	+10%	+10%	+7%
Southeast Asia	+45%	+45%	-13%

Table 1. SO2, NOx and PM emissions variations (related to 2016) as per IEA projections by 2040 [1].

As a result of the increasingly demanding legislation in force in most of the industrialized countries, the Internal Combustion (IC) engine industry is facing significant challenges, among which are both the reduction of pollutant emissions and the increase of thermal efficiency [2]. The combination of the previous demands with the widespread deployment of the IC engines derives in the imperative necessity of identifying continuous improvement measures, together with the optimization of the current production costs. Between the strategies considered by the IC engine sector it is noteworthy the search of alternative technologies to Spark Ignition (SI) and Compression Ignition (CI) conventional combustion modes, being the Homogeneous Charge Compression Ignition (HCCI) combustion one of the most promising options [3], even though several challenges still need to be addressed, jointly with other similar combustion modes such as Premixed Charge Compression Ignition (PCCI) and Reactivity Controlled Compression Ignition (RCCI) [4].

HCCI combustion is typically characterized by a lean mixture between air and fuel, reaching a significant degree of homogeneity before the start of combustion, which happens as an auto-ignition, without the participation of external agents. Furthermore, this auto-ignition starts simultaneously in different points of the combustion chamber, randomly located, without the presence of a flame front according to the results derived from optical analysis [5] [6]. The previous characteristics make possible HCCI combustion to develop a very fast Heat Release Rate (HRR), with a small variation of volume. Additionally, HCCI combustion is compatible with relatively high compression ratios, similarly to CI

engines, due to the low risk of knocking. Other similarity with CI engines is the lack of relevant mechanical losses related to pumping loop. Finally, HCCI combustion is possible with wide-ranging variety of fuels [7], differently from conventional SI and CI engines.

Some of the previous mentioned characteristics, such as the fast combustion, the high compression ratio and the minimization of the mechanical losses, allow HCCI combustion to reach relatively high thermal efficiencies, comparable to the conventional CI engines [8] [9]. Moreover, the significant degree of homogeneity needed to perform HCCI combustion avoids the existence of rich areas, which means the practically absence of particulate matter, equivalently to current SI engines. Finally, the non-existence of very high temperature areas, as a result of the mentioned homogeneous charge, lean mixture and lack of flame front, results in a significant cutback of the nitrogen oxides (NOx). The referred advantages provide HCCI combustion with a potential attractive compared to conventional SI and CI engines.

However, HCCI combustion drawbacks are significant, limiting its current commercial implementation. The main disadvantages consist on the difficulties related to the control of the start of combustion, since it is not triggered by external agents [10], and the limitations to the operation range in HCCI mode. On one hand, low loads derive in high emissions of unburned hydrocarbons (UHC) and carbon monoxide (CO) [8], due to the lack of thermal energy to promote the complete combustion of fuel [11]. Apart from incomplete combustions, low loads are related to slow heat release rates, with significant variations of volume, which penalize thermal efficiency. On the other hand, high loads in engines under HCCI operation mode are characterized by significant emissions of NOx, due to the high temperatures derived from fast heat release, which are accompanied by an undesired advance in the start of combustion, high pressure gradients, noise and knocking [12] [13] [14], all of them representing a risk for the mechanical integrity of the IC engines. Finally, cold start difficulties are also referred as one of the typical disadvantage of HCCI combustion, since the chamber walls are cold, which maximizes the heat losses from the air-fuel mixture, preventing auto-ignition to happen.

Focussing on the particular research necessities related to the HCCI combustion three main topics are typically referred: firstly, optical analysis to provide a better understanding about the phenomena that take place within the combustion chamber, secondly, numerical modelling to perform high quality simulations oriented to identify the parameters influencing the mentioned phenomena and, finally, control systems to optimize HCCI combustion performance in terms of power and pollutant emissions [15]. Intrinsically related to the second topic, numerical modelling, the present work describes the elaboration of a predictive tool consisting on a phenomenological multi-zone model, applicable to the simulation of HCCI combustion of both diesel and biodiesel fuels. Multi-zone models have demonstrated, after proper calibration, the capability of generating accurate predictions for IC engines, while not demanding significant amounts of resources. Based on the proposed model flexibility and low computational cost, additionally to the contribution to the simulation field, the work developed by the authors is created with the aim to be applied in the future to the development and testing of new improvement strategies oriented to overcome HCCI combustion current limitations, also mentioned previously as a major research demand.

3. Material and methods

3.1. Experimental methodology

The empirical basis of this work has been developed using a DEUTZ FL1 906 unit, a single cylinder, four-stroke, naturally aspirated, direct injection diesel engine, whose main rated characteristics are shown in Table 2. However, the unit configuration was modified in order to allow HCCI combustion operation mode:

- Introduction of an external Exhaust Gas Recirculation (EGR) system. Recirculated combustion gases were cooled down to ambient temperature before mixing with the fresh air flow not to promote combustion advancement of diesel and similar fuels with high cetane number, as a consequence of the so-called thermal effect of external EGR.

- Modification of the Start Of Injection (SOI) and Compression Ratio (CR). Two different configurations (early HCCI and late HCCI) were used experimentally, as described by Jiménez at al [16]. Early HCCI configuration was characterized by CR of 15:1 and SOI 45º BTDC, while CR of 18.4:1 and SOI 10º BTDC was used in late HCCI configuration. Although less attractive in terms of efficiency, late HCCI configuration was required in order to allow the use of biodiesel in HCCI combustion mode. Otherwise, mechanical damages happen even after a few hours of operation as a consequence of the physical-chemical properties of biodiesel, which hinder the vaporization of liquid fuel and lead to fuel deposition in cylinder walls. Summarizing, late HCCI configuration presented the only advantage of allowing the continuous use of biodiesel, not possible with the early HCCI configuration. Based on this fact, no switching mode between both configurations was considered.

- Optimization of the bowl-in-piston geometry as a measure to enhance turbulent mixing. The achievement of high swirl ratios before the start of combustion was an essential requirement to satisfactorily perform with the late HCCI setup [17].

- Increase of injection maximum pressure up to 650 bar, which leads to shorter injection periods, faster fuel evaporation and more homogeneous fuel-air mixtures.

The described modified IC engine was installed in a test bench belonging to the University of Seville, which, as shown in Figure 1, was equipped with electrical dynamometer to control both speed and load, exhaust gases analyser, high frequency data acquisition system and different gauges and transmitters, such as chamber pressure or instantaneous torque.

Tests were developed using diesel EN590 (B0) and rapeseed biodiesel (B100). Mixtures of diesel and 30% (B30) and 65% biodiesel (B65) were also considered. Although two setups have been previously referred, early HCCI configuration was only feasible with B0 fuel. For each fuel mixture, different conditions of speed, load and external EGR were considered. Regarding external EGR, for given speed and fuel flow, the fraction of recirculated gases

was increased in each test, until the external EGR caused the erratic operation of the engine, when a different set of speed and fuel flow was analysed.

As part of the experimental methodology, the combustion resulting from the combination of the above mentioned modifications and operating conditions was checked to truly correspond to a HCCI process. Firstly, pollutant emissions were analysed, satisfactorily resulting in the practically absence of particulate matter and in a drastic reduction of NOx levels. Additionally, the resulting HRR curve for each case was studied. Results, derived from the application of a single-zone model, show a very fast combustion, where only one mode or peak was identified, differently from conventional CI combustion, where two modes (pre-mix and diffusive) are present. Figure 2 shows the HRR curve related to one of the tested operating conditions. Those evidences confirm the analysed motor to be working under truly HCCI combustion conditions.

Type	DI 4-stroke one cylinder
Cylinder displacement	708 cm3
Bore	95 mm
Stroke	100 mm
Compression ratio	19:1
Piston	Bowl-in-piston
Maximum power	11 kW @ 3000 rpm
Maximum torque	45 N·m @ 2100 rpm
Number of injector holes	5
Injector holes diameter	0.26 mm
Injection pump	Mechanically driven
Injector nozzle opening pressure	240 bar
Injector maximum pressure	450 bar
Injector cone angle	120º
Lube oil pump	Mechanically driven
Inlet valve opening	1º BTDC
Inlet valve closing	36º ABDC
Inlet valve diameter	44.08 mm
Exhaust valve opening	36º BBDC
Exhaust valve closing	1º ATDC
Exhaust valve diameter	38.02 mm
Valve lifting	12 mm
Cooling system	Air (fan driven by flywheel)

Table 2. DEUTZ FL1 906 unit main rated characteristics.

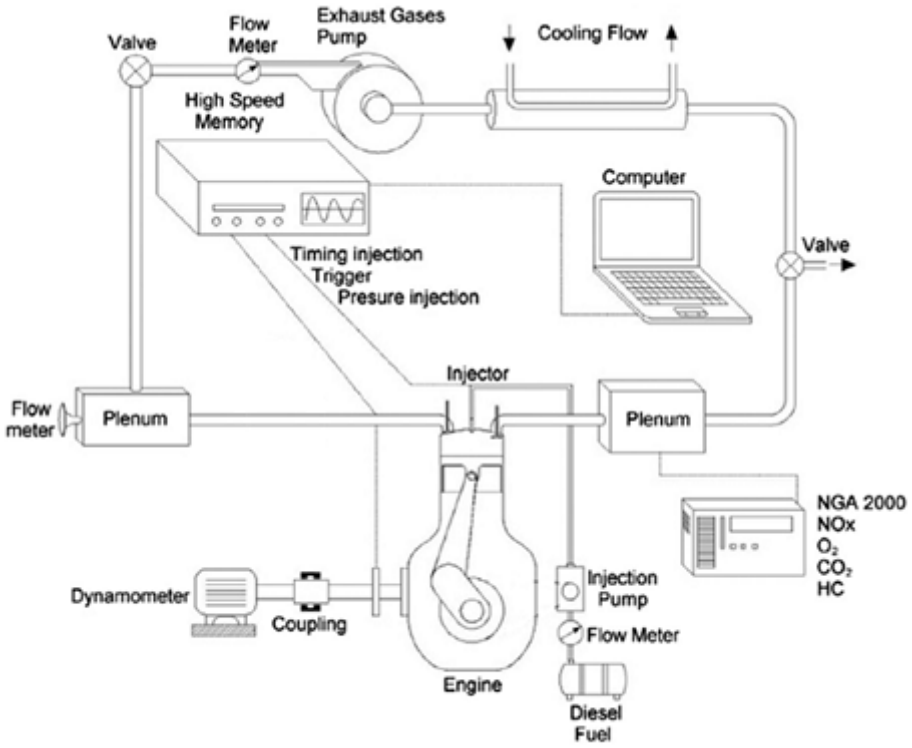

Figure 1: Schematic test bench.

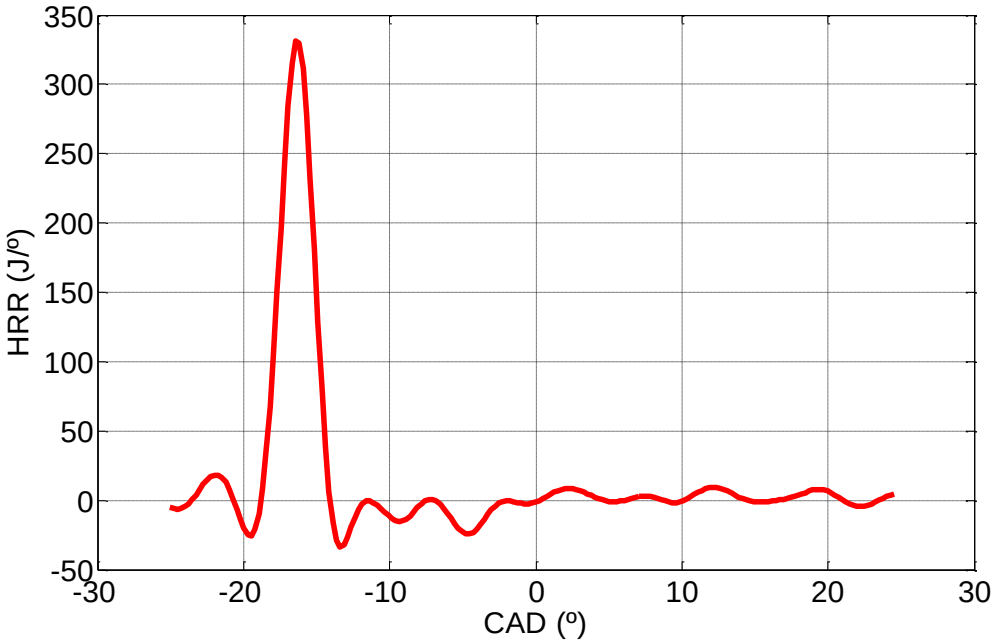

Figure 2: HRR evolution of early HCCI configuration with B0, 2100 rpm, 20 N·m and 0% external EGR.

3.2. Phenomenological model

The predictive tool presented here is based on a phenomenological multi-zone model described by Vélez et al. [18]. The mentioned model was developed to better simulate HRR in HCCI combustion by the consideration of no homogeneous areas within the combustion chamber, without significantly increasing the amount of required computational resources, as in models based on Computational Fluid Dynamics (CFD) codes. In order to model heterogeneities in both temperature and chemical composition fields the combustion chamber is discretized in different elementary homogeneous zones. Each of these sub-volumes, whose number is customizable according to user needs, is characterized considering a specific spatial location, which determines the physical processes happening within each boundary limit. Among those processes, the mentioned multi-zone model considers the existence of mass exchange between adjacent sub-volumes, heat losses to combustion chamber walls and mass losses to the crankcase.

Since the number of sub-volumes considered by the model is adjustable, the number of variables and equations involved in a simulation is also varying. However, although the model considers the existence of different temperatures and chemical compositions in each sub-volume, only a unique pressure, homogeneous for the complete combustion chamber, is accounted. The balance between the variables and the equations involved in the multi-zone model, with $(4+S)\cdot N$ freedom degrees, is shown Table 3, where N depicts the number of sub-volumes and S the number of chemical species involved in the combustion.

For this purpose, the combustion chamber was discretized in concentric cylinders (Figure 3), whose number was derived from a parametric study of the opposed effects of simulation error and required computational time. As known, the increase of the number of sub-volumes results in a reduction of the deviations related to the simulation results. However, this positive effect is neutralized by the increase of computational time required to complete the simulations. A study was developed using the number of sub-volumes as parameter, resulting in 10 sub-volumes to be the optimal figure for this configuration. Figure 4 shows the dimensionless error (both maximum error and

mean quadratic error) and computational time for one set of tested operating conditions (computed in a 2.67 GHZ CPU using “ode45” single-step solver by Matlab [19]), covering the previously mentioned behaviours. Finally, the relative size of the different sub-volumes was based on the distribution proposed by Aceves et al. [20], which uses one half of the sub-volumes to represent the 5% of the combustion chamber volume.

As previously mentioned, the multi-zone model developed by the authors is phenomenological, since both ignition delay and combustion development are governed by a set of two functional laws (Equations 1 & 2).

$$\tau_i = A_D \cdot \rho_i^{B_D} \cdot [O_2]_i^{C_D} \cdot [Fuel]_i^{D_D} \cdot EXP\left(\frac{E_D}{R_i \cdot T_i}\right) \qquad \text{Equation 1.}$$

$$\dot{M}_i^{REA}\Big|^{FUEL} = A_C \cdot \rho_i^{B_C} \cdot [O_2]_i^{C_C} \cdot [Fuel]_i^{D_C} \cdot EXP\left(\frac{E_C}{R_i \cdot T_i}\right) \quad \text{Equation 2.}$$

Where, A_D, B_D, C_D, D_D and E_D are the five constants required to characterize ignition delay law; A_C, B_C, C_C, D_C and E_C denote the five constants required to characterize combustion development law; ρ is the density; $\cdot[O_2]$ and $\cdot[Fuel]$ are oxygen and fuel concentration, respectively; R is the gas constant, T is the temperature; τ_i refers to ignition delay; $\dot{M}_i^{REA}\Big|^{FUEL}$ is the fuel combustion rate and, finally, the subscript i refers to the i-th sub-volume.

Although the mentioned coefficients (A, B, C, D and E) are identical for all the sub-volumes, the heterogeneity in terms of both temperature and chemical composition between different locations derives in the independent evolution of each different sub-volume. This characteristic allows the heat release not to take place simultaneously in the whole combustion chamber, as in single-zone models.

Finally, although the terminology NOx includes both nitrogen monoxide (NO) and nitrogen dioxide (NO2) emissions, the firsts are predominant over NO2 emissions in IC engines, reaching NO2 maximum rates even of 15% compared to NO emissions in CI engines [21]. Based on this, in the present work NOx

emissions are considered through a NO emissions model, which are mainly generated from the molecular nitrogen oxidation. Specifically, the extended Zeldovich mechanism (equations from 3 to 5) has been adopted [22] [23]:

$$O + N_2 \overset{1}{\longleftrightarrow} NO + N \qquad \text{Equation 3.}$$

$$N + O_2 \overset{2}{\longleftrightarrow} NO + O \qquad \text{Equation 4.}$$

$$N + OH \overset{3}{\longleftrightarrow} NO + H \qquad \text{Equation 5.}$$

Reaction rates corresponding to each of the previous reactions can be obtained from different sources, being used in this work the figures provided by Heywood [21], together with the following assumptions by the same author:

- Considering that the monoatomic nitrogen concentration is significant lower than the other species involved in the mechanism, this substance is considered to be in equilibrium and its concentration to be in steady-state.
- Since NO formation after combustions is higher than the formation during this period, NO formation is assumed to be decoupled from combustion and O, O2, OH, H y N2 concentrations are approximated by their equilibrium concentrations.

Variables	
1	Chamber pressure
N	Sub-volume temperatures
N	Sub-volume overall masses
N-1	Masses exchanged between adjacent sub-volumes
S·N	Sub-volume chemical species masses
N	Ignition delay
Equations	
N	First law of thermodynamics
N	Thermal state equation
N	Mass balance
S·N	Chemical species mass balance
N	Ignition delay functional law

Table 3: Variables and equations balance.

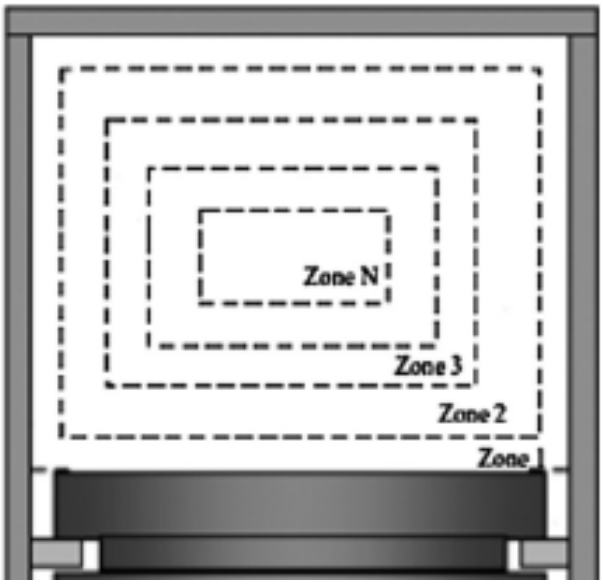

Figure 3: Combustion chamber discretized in concentric cylinders.

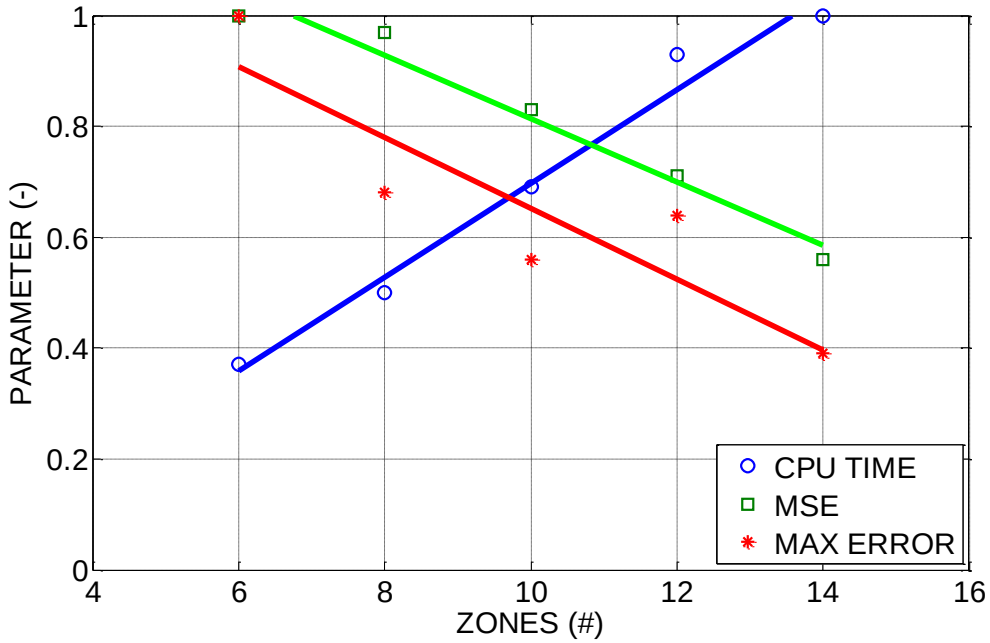

Figure 4: Dimensionless error and computational time for early HCCI configuration with B0, 2100 rpm, 15 N·m and 36% external EGR.

3.3. Predictive tool

Despite the lack of a kinetic mechanism to reproduce the fuel combustion, the phenomenological model described in the previous section demonstrated to actually constitute a valid and useful tool to numerically simulate HCCI combustion, based on the accuracy of the obtained results in comparison with

the recorded experimental data [18]. However, the functional laws used to model the fuel combustion were calibrated for those operational conditions tested experimentally (speed from 1200 to 2400 rpm and equivalence ratio from 0.2 to 0.6). The mentioned calibration consisted in the optimization, for each available experimental test, of the scaling coefficients in both ignition delay and combustion development laws, A_D and A_C respectively. The referred calibration consisted in the minimization, for each experimental test, of the mean quadratic error between the simulated and the experimental pressure curves. This approach was valid to obtain simulations under the same operative conditions as in the experimental tests, but does not allow establishing predictions in conditions different from those. Consequently, in order to create a tool able to predict the performance of an IC engine under HCCI combustion conditions without the necessity of running experimental tests, the development of an analytical structure for both ignition delay and combustion development functional laws is required.

The methodology applied to build the analytical structure of the predictive model will be based on the multidimensional response surface generated during the calibration of the scaling coefficients involved in the phenomenological model. From those surfaces, different models comprising polynomial functions based on different regression variables will be obtained for both A_D and A_C scaling coefficients. Quadratic polynomials, including variable interactions, with coefficients obtained by least squares method were considered by the authors to model A_D and A_C .

Summarizing, the challenge to obtain a predictive tool from the previous phenomenological model is to generate an analytical mechanism that, given a set of regression variables representing the engine operative conditions, provides the user with the optimal figures for the scaling coefficients needed to particularize both the ignition delay and the heat release rate functional laws, which rule the combustion development in the proposed multi-zone model for HCCI engines. By applying this procedure, simulating HCCI engines performance without experimental testing is possible within a specific range, after proper calibration.

The significant number of parameters involved in the previously mentioned experimental tests results in the identification of proper regression variables being a relatively complex task. Taking into consideration the methodology followed to obtain the experimental data, the magnitudes chosen by the authors as regression variables are equivalence ratio (x_1), rotational speed (x_2) and external EGR fraction (x_3). Additionally, for the predictive models related to the late HCCI configuration, biodiesel fraction is also considered as a regression variable (x_4), since, apart from the previously mentioned variables, different fuel blends were used during the experimental stage. On the other hand, as mentioned, early HCCI configuration was possible only using diesel fuel, so no regression variable to describe fuel characteristics was required in this case. Other typical parameters were not considered as regression variables because they were not modified during the experimental testing, such as compression ratio or the injection system characteristics. Ambient conditions were also not considered as regression variables because only minor variations were noticed between the different experiments, since they were developed within the same closed test bench, with a high air renovation and during a relatively short interval of time. Equation 6 shows an example of the polynomial used to predict parameter "y", adapted to four regression variables (x_i), which involves fifteen coeficients (k_i).

$$y = k_0 + k_1 \cdot x_1 + k_2 \cdot x_2 + k_3 \cdot x_3 + k_4 \cdot x_4 + k_5 \cdot x_1 \cdot x_2 + k_6 \cdot x_1 \cdot x_3 + k_7 \cdot x_1 \cdot x_4 + k_8 \cdot x_2 \cdot x_3 + k_9 \cdot x_2 \cdot x_4 + \\ + k_{10} \cdot x_3 \cdot x_4 + k_{11} \cdot x_1^{\,2} + k_{12} \cdot x_2^{\,2} + k_{13} \cdot x_3^{\,2} + k_{14} \cdot x_4^{\,2} \qquad \text{Equation 6.}$$

By applying the described methodology, two polynomials, one for the early HCCI configuration (3 variables and 10 coefficients) and other for the late HCCI configuration (4 variables and 15 coefficients), were obtained for each scaling coefficient in both ignition delay and combustion development laws, A_D and A_C. Finally, Table 4 shows the results obtained using least squares method for the coefficients involved in the regression polynomials modelling scaling coefficients A_D and A_C.

	Early HCCI		Late HCCI	
	A_C	A_D	A_C	A_D
k0	-7.94E+3	1.24E-2	1.91E+2	-6.06E-2
k1	5.65E+0	-1.66E-5	1.48E+1	1.67E-1
k2	1.57E+4	2.51E-2	-1.91E-1	1.30E-4
k3	8.01E+2	-2.20E-2	3.19E+2	-9.48E-2
k4	-6.28E+0	-7.30E-6	-7.32E+2	-1.81E-1
k5	-8.65E-1	8.49E-6	2.24E-2	-1.31E-4
k6	-2.28E+3	1.23E-2	-8.38E+1	1.90E-1
k7	-7.01E-4	5.56E-9	-1.57E+2	-6.67E-2
k8	-5.76E+3	-1.60E-2	-4.67E-1	7.32E-5
k9	1.41E+3	2.68E-2	3.05E-1	9.06E-5
k10	-	-	-2.32E+2	-5.63E-2
k11	-	-	-2.59E+1	7.56E-2
k12	-	-	9.33E-5	-3.79E-8
k13	-	-	6.43E+2	-7.94E-2
k14	-	-	9.88E+2	7.05E-2

Table 4: Multiple regression results for scaling coefficients in both ignition delay and combustion development functional laws, A_D and A_C.

4. Validation and results

Before discussing the predictive model validation, it is noteworthy that the obtained results reinforce the previously mentioned decision of developing independent polynomial models for the two analysed configurations, early HCCI and late HCCI. This statement is based on the different, or even opposite, trend experienced by the scaling coefficients A_D or A_C with respect to same regressive variable for the mentioned configurations. This implies that, in case of not distinguishing between configurations, the unification of the early HCCI and late HCCI polynomials would have resulted in higher errors related to the predictions derived from the multi-zone model. Specifically, regarding A_C coefficient model, the regression variable with a higher impact is external EGR fraction for both early HCCI and late HCCI. However, the trend is opposite in each case, since the relationship is direct for late HCCI experiments and indirect for early HCCI ones.

The methodology followed to validate the proposed predictive multi-zone model consists on the comparison between chamber pressure curve derived from the

simulations and experimental data. Although the final purpose of the proposed predictive multi-zone model is to capture the allowable performance of an IC engine under HCCI conditions, Figures from 5 to 10 quantitatively illustrate the mentioned comparison. As derived from the referred figures, the proposed predictive model matches the actual behaviour of the analysed IC engine under HCCI combustion conditions, reproducing the fundamental effects of the combustion process and allowing, among others, the simulation of the pressure gradient decrease when increasing cooled external EGR fraction, the start of combustion delay when increasing cooled external EGR fraction or, apparently, when increasing rotational speed and, finally, the start of combustion advancement when increasing the biodiesel fraction. The overall analysis of the obtained results for the early HCCI configuration states the predictive model tendency to anticipate the start of combustion compared to the experimental data, although the results regarding maximum pressure and pressure gradient are excellent. The mentioned tendency to anticipate the start of combustion by the predictive model is illustrated in Figures 5 and 6, where the predicted curve is generally anticipated to the experimental measurement within the interval related to the start of combustion. On the other hand, the results derived from the predictive model for the late HCCI configuration denotes a good agreement for the start of combustion between simulated and experimental data, as well as for the pressure gradient. Contrarily, the predictive model developed for the late HCCI configuration faces the bigger deviations regarding the estimation of the maximum pressure, which results over-predicted. Although this behaviour can be observed in Figures 7 (B0) and 8 (B30), the maximum pressure over-prediction is more evident in Figure 9 (B65). Despite the previous statement regarding maximum pressure over-prediction, Figure 10 (B100) shows the opposite effect for high levels of external EGR. This trend is attributable to the statistical deviation caused by the use of figures close to the upper limit of regression variables such as external EGR and biofuel fractions.

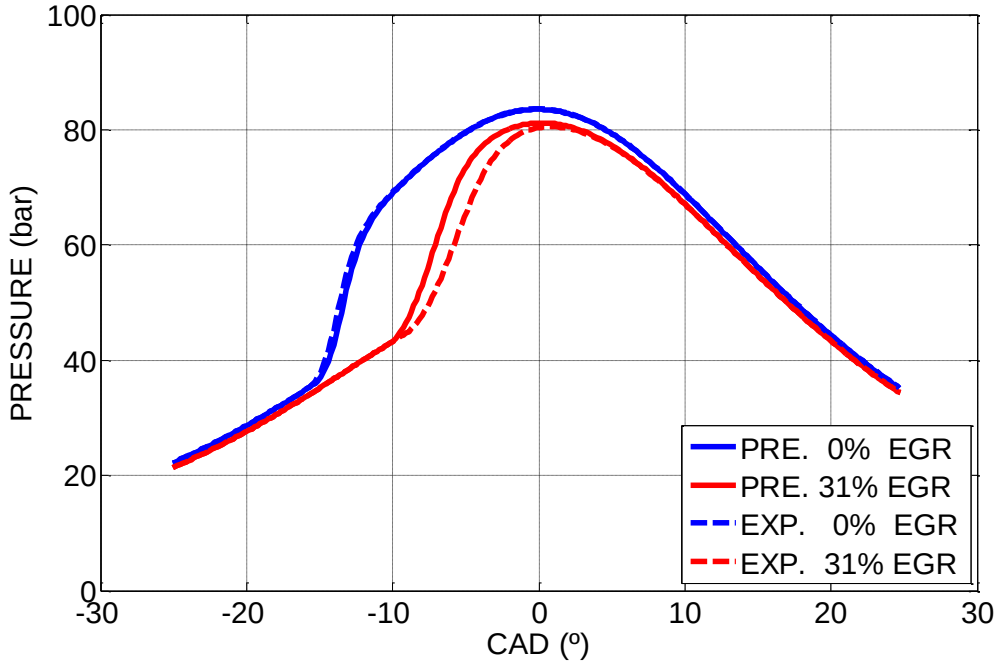

Figure 5: Comparison between the predictive multi-zone model and the experimental data. Pressure evolution for diesel fuel (B0), with early HCCI configuration, 1500 rpm and equivalence ratio 0.34.

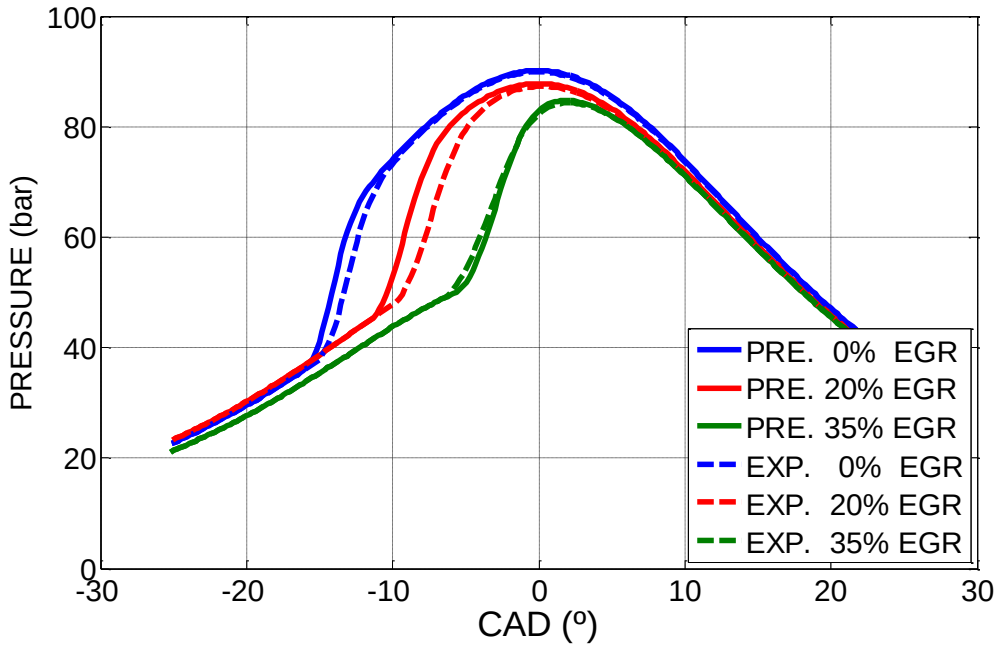

Figure 6: Comparison between the predictive multi-zone model and the experimental data. Pressure evolution for diesel fuel (B0), with early HCCI configuration, 1800 rpm and equivalence ratio 0.34.

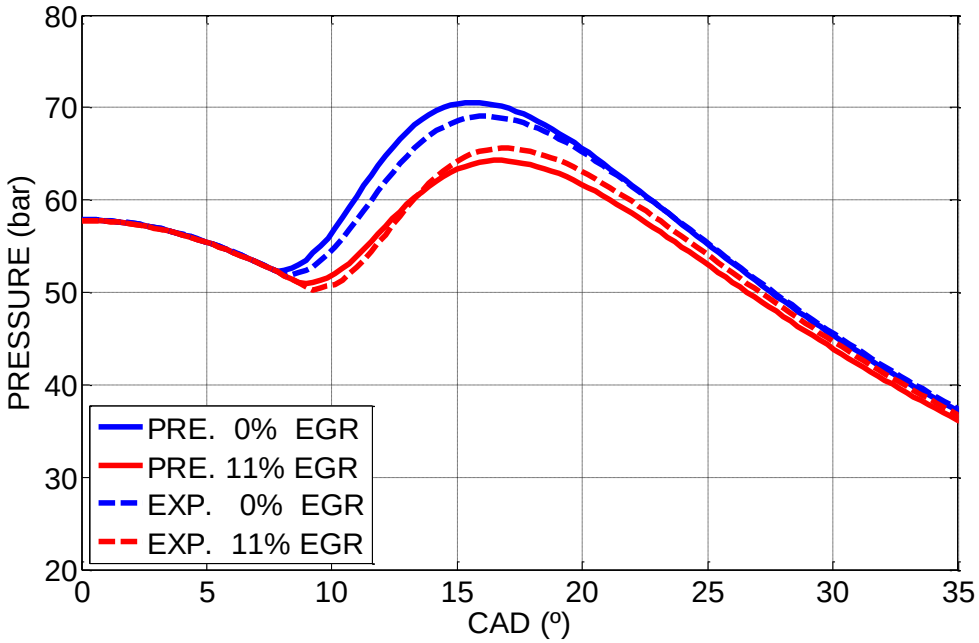

Figure 7: Comparison between the predictive multi-zone model and the experimental data. Pressure evolution for diesel fuel (B0), with late HCCI configuration, 2400 rpm and equivalence ratio 0.60.

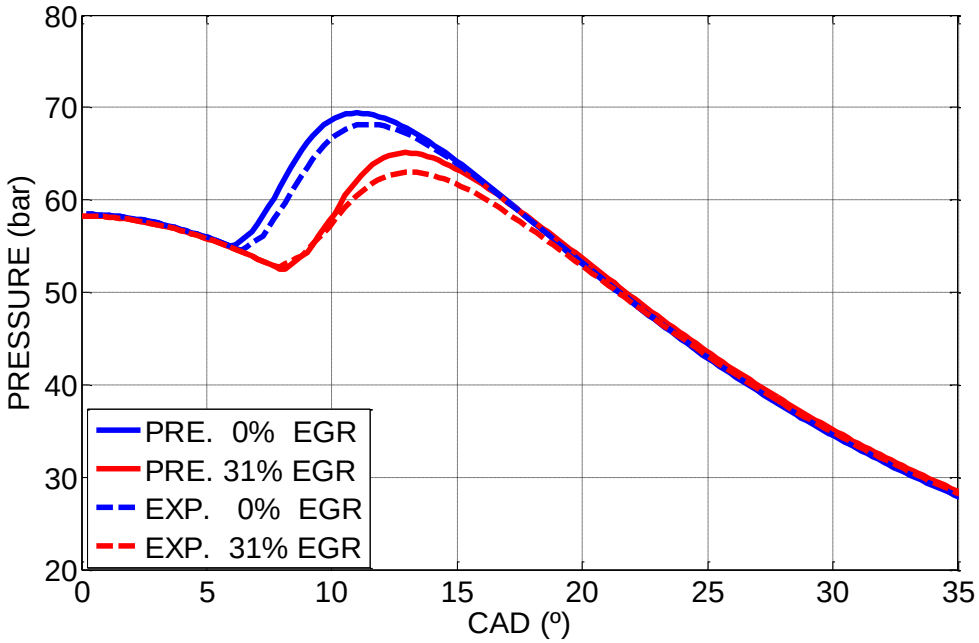

Figure 8: Comparison between the predictive multi-zone model and the experimental data. Pressure evolution for diesel fuel and 30% biodiesel (B30), with late HCCI configuration, 1800 rpm and equivalence ratio 0.20.

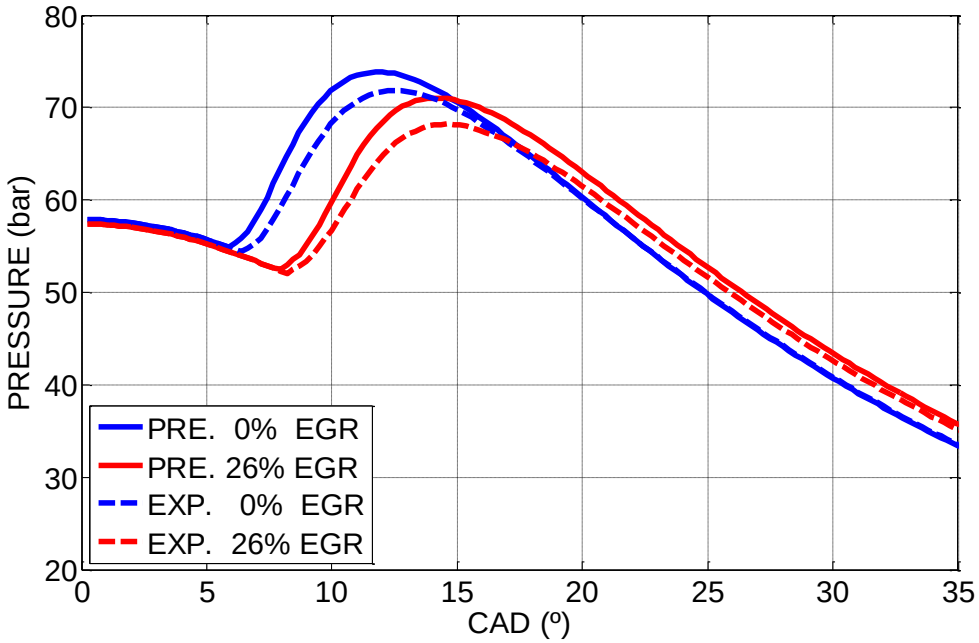

Figure 9: Comparison between the predictive multi-zone model and the experimental data. Pressure evolution for diesel fuel and 65% biodiesel (B65), with late HCCI configuration, 2100 rpm and equivalence ratio 0.45.

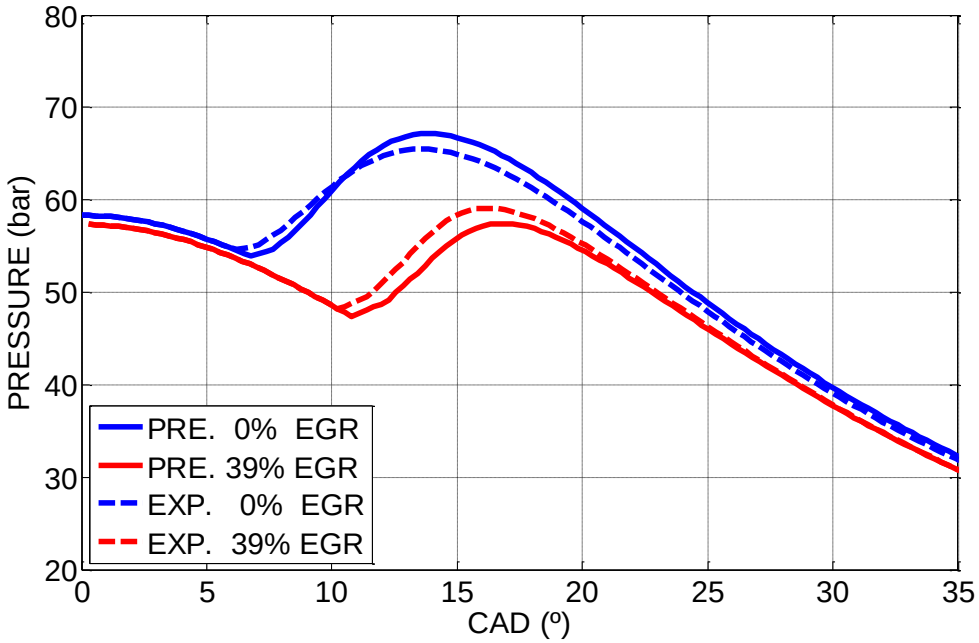

Figure 10: Comparison between the predictive multi-zone model and the experimental data. Pressure evolution for biodiesel fuel (B100), with late HCCI configuration, 2400 rpm and equivalence ratio 0.45.

To complete the validation of the predictive multi-zone model derived from the application of the methodology shown in the previous section, errors obtained in

predicting the chamber pressure curve were analysed. Both the maximum error (absolute value of the higher difference between the simulated pressure curve and the experimental one, considering the same crankshaft angle degree for both of them) and the maximum pressure error (absolute value of the difference between the maximum of the simulated pressure curve and the maximum of the experimental one, independently of considering the same crankshaft angle degree for both of them or not) were assessed. The average figures related to the two mentioned errors are shown in Table 5, distinguishing between the two different configurations analysed. Figures related to the early HCCI configuration resulted in higher maximum errors than late HCCI configuration. Additionally, despite the relatively high value of the average maximum error for early HCCI configuration, this has no impact over the general results, since this deviation takes place during the early stage of the combustion, where, due to the slightly gap between predicted and experimental curves, the maximum error is accumulated. However, this deviation is rapidly corrected once the combustion is triggered in the predictive model. In other words, the maximum error related to the early HCCI configuration is attributable to the previously mentioned tendency of the predictive model to anticipate the start of combustion compared to the experimental data. Contrarily, the trend is opposite regarding the maximum pressure error, since results related to the early HCCI configuration allow obtaining lower deviations than for the late HCCI configuration.

Furthermore, the accuracy of the proposed model in relation to maximum pressure estimation (refer to Table 5) represents also a relevant aspect of the present work, since maximum pressure conditions gases maximum temperature, which in turn conditions NOx emissions. Additionally, the capability of properly modelling maximum pressure provides the model with an added value, since the proposed model could be used in Heavy Duty Diesel (HDD) applications. HDD engine sector faces currently the necessity of improvements regarding specific power, which requires the increase of combustion chamber maximum allowable pressure, which will reach figures of 250 bar according to estimations [24]. The mentioned maximum allowable pressure increase requires the development of structural detailed analyses during design stage, which will

demand a proper estimation of the maximum combustion chamber pressure in different operation regimes.

Configuration	Mean maximum error (bar)	Mean maximum pressure error (bar)
Early HCCI	7.58	1.23
Late HCCI	3.70	1.98

Table 5: Average errors derived from predictive model validation.

The main application of the proposed predictive multi-zone model consists on the mechanical pre-design of off-road IC engines, with characteristics similar to those shown in Table 2. For this reason, after checking the validity of the analytical structures used to characterize both the ignition delay and the combustion development functional laws, hereafter an example of the potential uses of the proposed multi-zone model is illustrated. The aim of this example is to provide an evidence of the capabilities of the proposed model to be used as a predictive tool applicable to the analysis of small cylinder displacement off-road engines under HCCI conditions. According to this approach, the operational maps, related to both Brake Specific Fuel Consumption (BSFC) and NOx emissions will be characterized for early HCCI configuration, using Brake Mean Effective Pressure (BMEP) and rotational speed as main axes. The selection of BSFC and NOx emissions is oriented to capture, not only the engine efficiency, but also the NOx emissions drastic reduction derived from HCCI combustion, which constitutes one of the main attractions of this technology over conventional CI engines. However, as shown on Equation 7, BMEP calculation requires, apart from obtaining indicated performance derived from multi-zone model, the introduction of a mechanical losses model. The model proposed by Heywood for CI engines was considered to characterize the mechanical losses [21]. Once the BMEP is defined, the brake power is calculated (Equation 8), which combined with the hourly fuel consumption allows BSFC calculation (Equation 9).

$$BMEP = IMEP - P_{Loss}^{Mech} \qquad \text{Equation 7.}$$

$$BMEP = \frac{W_B}{V_D} = \frac{P_B \cdot n_R}{V_D \cdot N} = \frac{T_B \cdot 2 \cdot \pi \cdot n_R}{V_D} \qquad \text{Equation 8.}$$

$$BSFC = \frac{\dot{m}_f}{P_B}$$ Equation 9.

Where, P_{Loss}^{Mech} refers to the mechanical losses equivalent pressure; W_B is the brake work; V_D is the engine displacement; P_B is the brake power; n_R refers to the revolutions per cycle (2 in a four-stroke engine); N is the rotational speed (rpm); T_B is the brake torque and, finally, $\dot{m}_f$ refers to the hourly fuel consumption.

The first conclusion derived from the obtained results is the considerable limitation to high load operation, reaching maximum BMEP around 3 bar despite the nominal CI configuration reaching 7 bar. The penalization over BMEP is caused by the ignition advance derived from load increase, which generates a combustion chamber heating effect. The ignition advance involves an increase in the negative work (work developed during the compression stroke). In other words, the combustion is initiated too early referenced to TDC, which penalizes the generated work. Regarding the BSFC results, similarly to BMEP, the resulting figures are values significantly higher than those corresponding to the original CI configuration (221.5 g/h/kW). Figure 11 shows BSFC related to certain conditions of load and rotational speed, depicting BSFC increase with the engine load, i.e. BMEP. As mentioned in relation to BMEP, the excessive ignition advance experienced at high loads implies a decrease in generated power due to the negative work, which dramatically impacts BSFC. Figure 12 shows the operational map corresponding to NOx emissions related to certain conditions of load and rotational speed, which, contrarily to BSFC, experiences a very significant reduction compared to a conventional CI engine due to the non-existence of very high temperature areas. Despite the mentioned reduction, Figure 12 shows that higher NOx emissions are experienced at high loads, as a consequence of the higher maximum temperature reached within the combustion chamber.

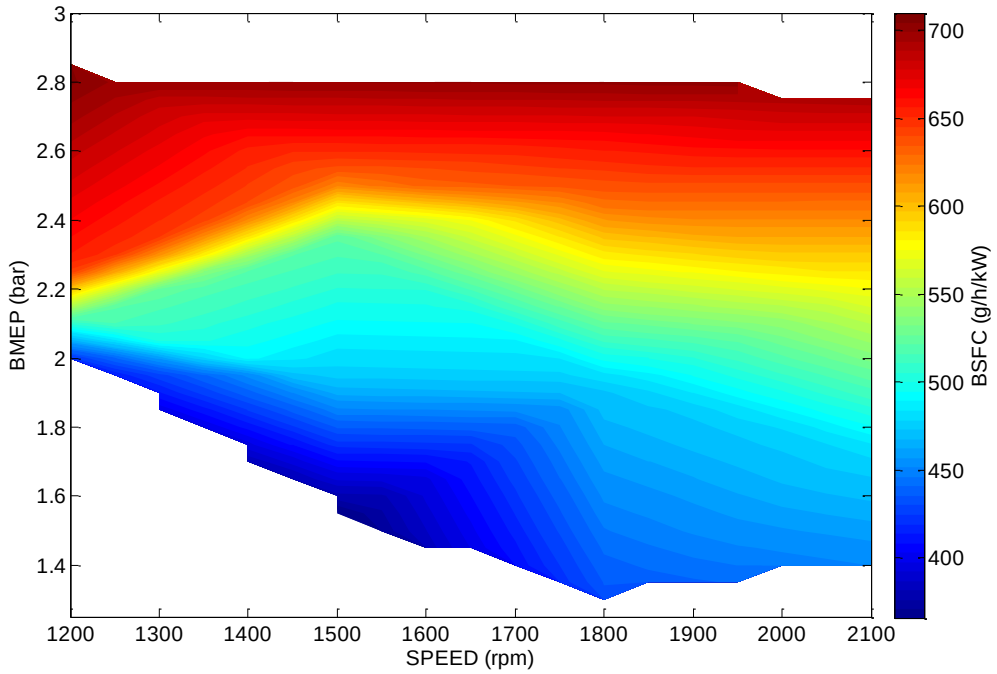

Figure 11: Simulated BSFC related to Deutz-Díter FL1 906 unit with early HCCI configuration (CR 15:1, SOI 45º BTDC).

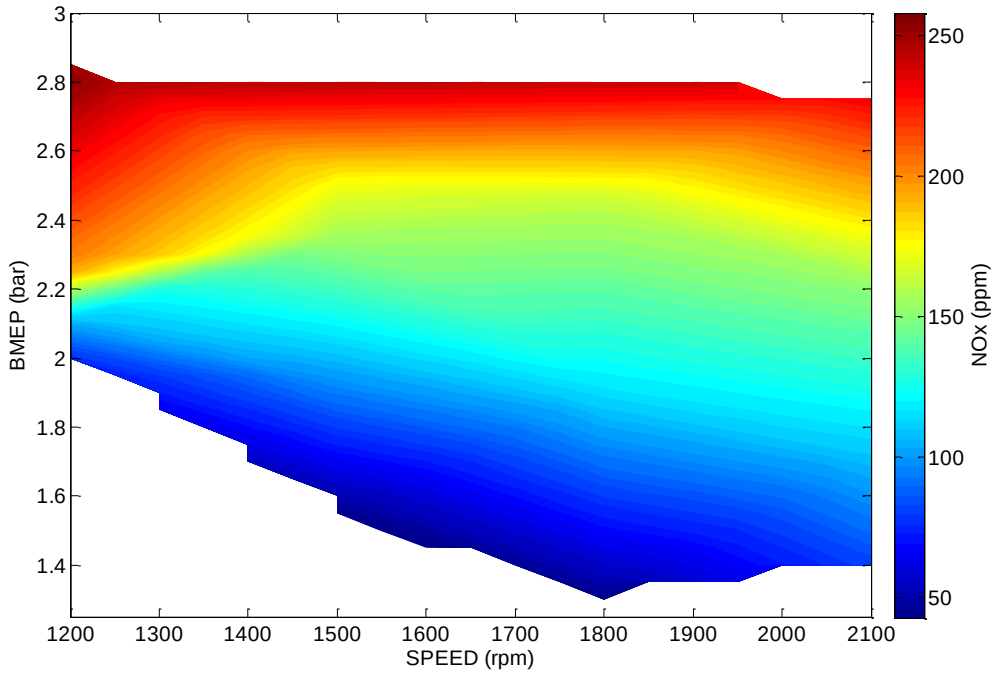

Figure 12: Simulated NOx emissions related to Deutz-Díter FL1 906 unit with early HCCI configuration (CR 15:1, SOI 45º BTDC).

After illustrating the poor performance in terms of efficiency experienced by the analysed engine working with early HCCI configuration, the necessity of optimizing its operation is confirmed. A reduction of the excessive negative work is needed to improve engine performance, which involves delaying the start of combustion, specifically at high loads. The use of cooled external EGR represents a typical mechanism to perform the mentioned delay of ignition [25]. This issue allows illustrating the advantages of the proposed predictive model, since, instead performing experimental tests that will cause economical and schedule impact, a numerical analysis based on the multi-zone model was performed. Applying this methodology, a battery of simulations was generated, allowing the identification of the external EGR fraction that maximized the generated toque for each condition of fed fuel and rotational speed. Figure 13 shows the results related to the optimal external EGR fraction related to certain conditions of load and rotational speed. The mentioned figure shows how the optimal external EGR fraction decreases when load is increased, in spite of the required delay being higher. The mentioned decrease of optimal external EGR fraction is a consequence of the higher content in combustions products generated at high loads, what increases the thermal capacity of the mix compared to fresh air.

As a consequence of the introduction of cooled external EGR, the negative work is considerably reduced due to the delay of the combustion start, which allows BMEP reaching figures 50% higher than in the previous scenario for high loads. Additionally, Figure 14 shows the significant reduction in BSFC, compared to Figure 11, when the optimal external EGR fractions are used, considering certain conditions of load and rotational speed. This reduction is derived from the higher power generated when the ignition occurs in the optimal crankshaft angle degree. Despite the relevant reduction of BSFC, the resulting figures still are over the reasonable limits for an optimized IC engine. Regarding NOx related to the optimal external EGR fraction, lower emissions result as a consequence of the decrease of chamber maximum temperature derived from both capacitive and dilutive effects of cooled external EGR [26] [27], as stated in Figure 15, which shows NOx emissions related to certain conditions of load and rotational speed, although the overall trend is quite similar to that shown in

Figure 12. Finally, Figure 16 shows a comparison between the operation limits related to the three different configurations mentioned in this section (CI, HCCI without external EGR and HCCI with external EGR). Two main conclusions derive from Figure 16. Firstly, the decrease of maximum BMEP of HCCI combustion compared with the conventional CI combustion, although this disadvantage is balanced by the attractive decrease of NOx emissions derived from HCCI combustion in comparison with CI combustion. The second conclusion consists on the beneficial effect of cooled external EGR over HCCI combustion, increasing maximum BMEP, as previously described. As a consequence of these conclusions related to the engine performance under different operation modes, the attractiveness of dual operation (CI/HCCI) is highlighted.

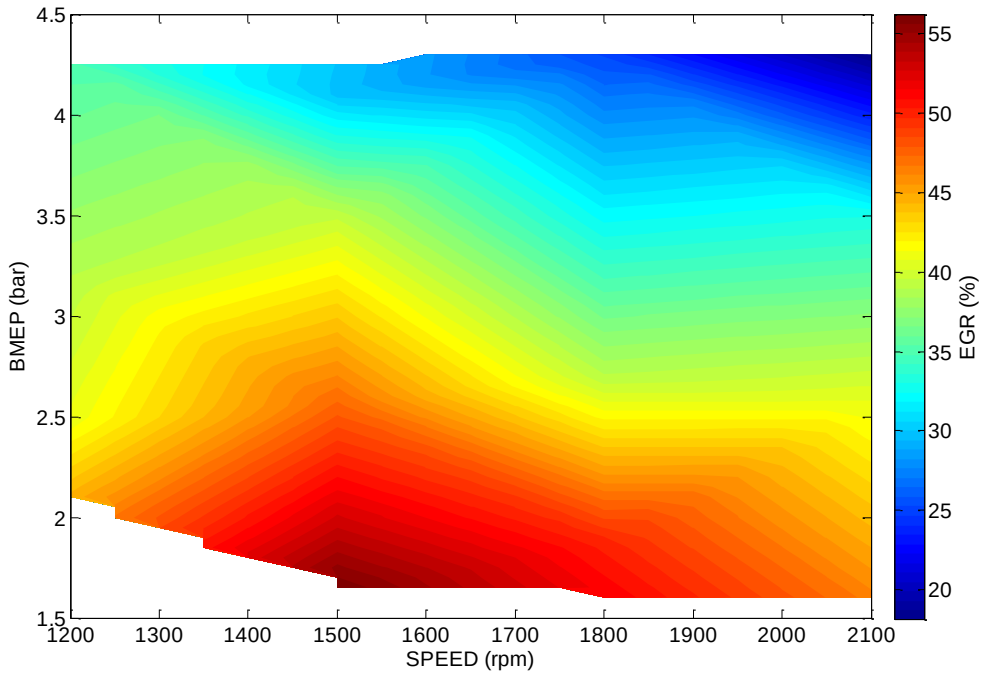

Figure 13: Simulated optimal external EGR fraction (maximum torque) related to Deutz-Díter FL1 906 unit with early HCCI configuration (CR 15:1, SOI 45º BTDC).

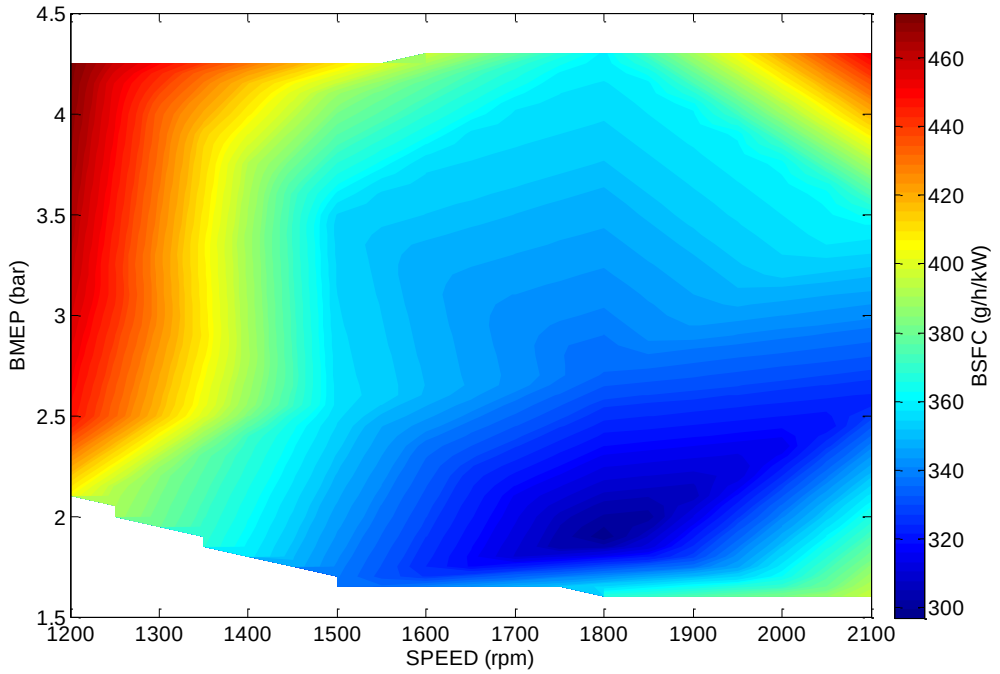

Figure 14: Simulated optimized BSFC related to Deutz-Díter FL1 906 unit with early HCCI configuration (CR 15:1, SOI 45º BTDC).

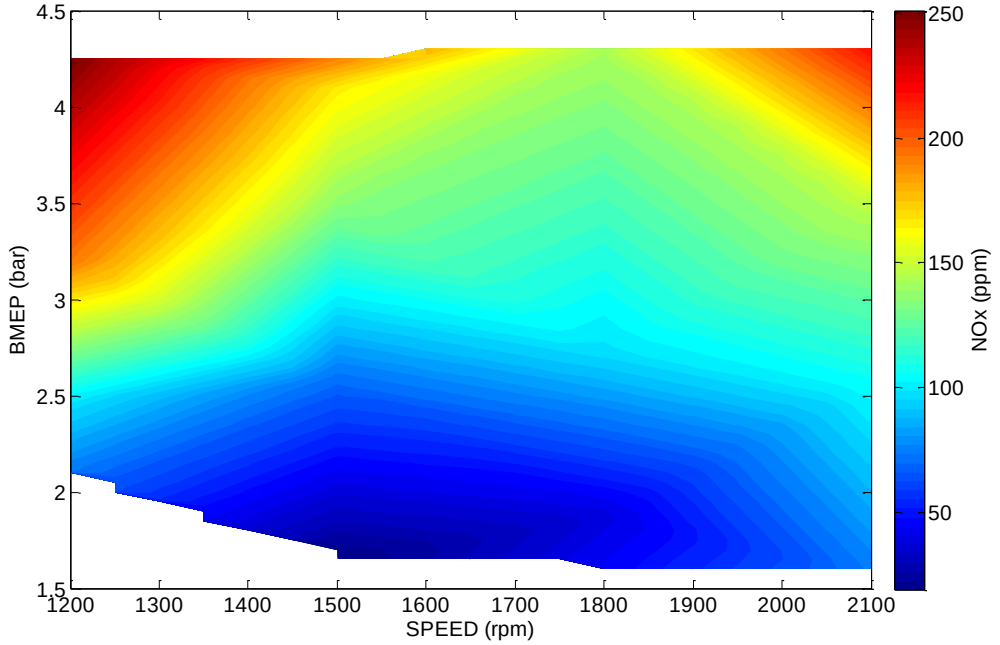

Figure 15: Simulated NOx emissions related to optimized BSFC of Deutz-Díter FL1 906 unit with early HCCI configuration (CR 15:1, SOI 45º BTDC).

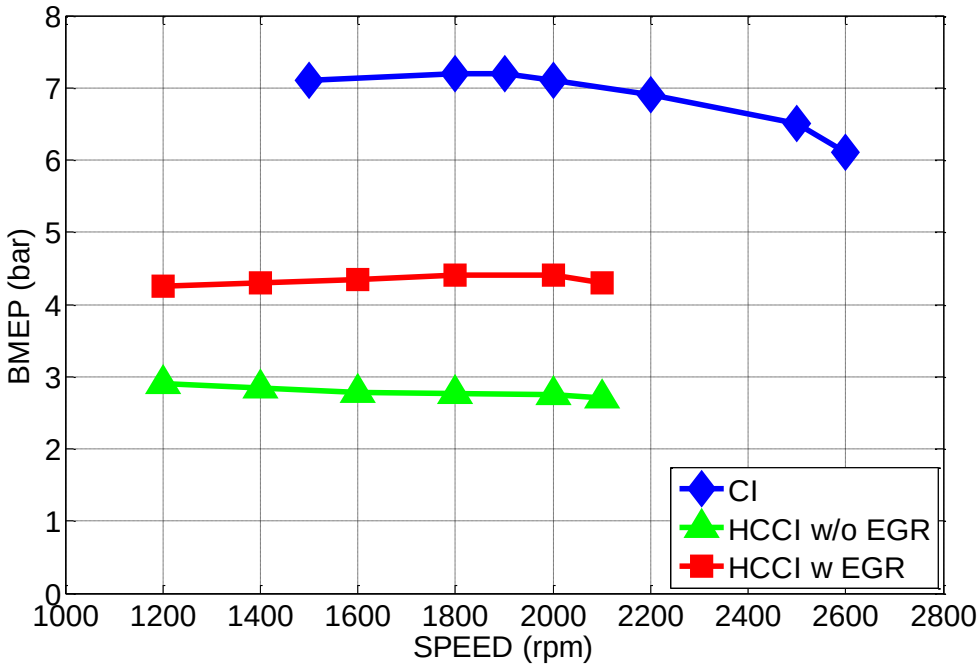

Figure 16: Operation limits in the engine map related to to Deutz-Díter FL1 906 unit.

5. Conclusions

The results shown in previous paragraphs attest the potential of the proposed multi-zone model to be used as a predictive tool applied to off-road engines analysis under HCCI conditions. Regarding the goodness of the results obtained using this model, the identified deviations are acceptable considering the advantages provided by the predictive tool, mainly consisting in the capability of performing simulations of different indicated parameters without the necessity of developing complex experimental studies. The proposed approach positively impacts the required resources in terms of both time and cost. Additionally, the lack of a kinetic mechanism to simulate fuel combustion has been satisfactorily overcome by the use of the proposed functional laws, modelling both ignition delay and combustion development.

Based on the HCCI combustion predictive capabilities, the proposed multi-zone model results highly useful in applications where the intensive collection of data related to the engine performance is required, compared to those processes based on experimental approaches. By this methodology, users are able to perform engine characterization during both pre-design and post-design stages,

with the intention to minimize costs related to experimentation in test benches. As an example of this potential uses, the authors have applied the proposed predictive model to define the optimal operation of a control strategy based on the addition of cooled external EGR. Using the proposed model an increase of 50% in BMEP and a reduction of 30% in BSFC have been achieved for high load operation. These results illustrate the application of the proposed model to the definition of optimized operation maps for HCCI engines, which results feasible by means of current electronic control systems. Based on these premises, next task performed by the authors will consist in the application of the proposed multi-zone model to the development of HCCI combustion new control systems.

6. Acknowledges

This work is part of item DPI2013-46485-C3-3-R within the R&D National Plan in the period 2013-2016 and has been backed by the Spanish Government (Ministry of Economy and Competitiveness). The authors are grateful for the support.

7. Nomenclature

General:

A	Scaling coefficients in both ignition delay and combustion development laws.
BMEP	Brake mean effective pressure.
BSFC	Brake specific fuel consumption.
BTDC	Before top dead centre.
CAD	Crankshaft angle degree.
CFD	Computational fluid dynamics
CI	Compression ignition.
CO	Carbon monoxide.
CR	Compression ratio.

EGR	Exhaust gas recirculation.
HCCI	Homogeneous charge compression ignition.
HDD	Heavy duty diesel
HRR	Heat release rate.
IC	Internal combustion.
k	Polynomial coefficient.
M	Mass.
$\dot{m}_f$	Hourly fuel consumption.
N	Rotational speed (rpm).
n_R	revolutions per cycle (2 in a four-stroke engine).
NOx	Nitrogen oxides.
P_B	Brake power.
P_{Loss}^{Mech}	Mechanical losses equivalent pressure.
PCCI	Premixed charge compression ignition.
R	Gas constant.
SI	Spark ignition.
SOI	Start of injection.
T	Temperature.
T_B	Brake torque.
TDC	Top dead centre.
UHC	Unburned hydrocarbons.
V_D	Engine displacement.
W_B	Brake work.

x	Regression variable.
y	Predicted variable.
ρ	Density.
τ	Ignition delay.

Subscript:

C	Related to the combustion development functional law.
D	Related to the ignition delay functional law

Superscript:

REA	Related to a chemical reaction.

8. References

[1] International Energy Agency. “Energy and Air Pollution. World Energy Outlook 2016. Special Report”. 2016.

[2] Stanton, D. "Systematic development of highly efficient and clean engines to meet future commercial vehicle greenhouse gas regulations". SAE Int. J. Engines. 2013. Vol. 6(3). doi:10.4271/2013-01-2421.

[3] Charalambides, A.G. “Advances in internal combustion engines and fuel technologies” (Chapter 4: Homogeneous charge compression ignition (HCCI) engines.). Edited by Hoon Kiat Ng. ISBN 978-953-51-1048-4, 318 pages, Publisher: InTech, Chapters published March 20, 2013.

[4] Reitz R, Duraisamy G. “Review of high efficiency and clean reactivity controlled compression ignition (RCCI) combustion in internal combustion engines”. Progress in Energy and Combustion Science. 2015. Vol. 46: 12-71.

[5]Noguchi M, Tanaka T, Takeuchi Y. “A study on gasoline engine combustion by observation of intermediate reactive products during combustion”. SAE paper 790840. 1979.

[6] Aoyama T, Hattori Y, Mizuta J, Sato Y. “An experimental study on premixed charge compression ignition gasoline engine”. SAE paper 960081. 1996.

[7] Christensen M, Hultqvist A, Johansson B. “Demonstrating the multi fuel capability of a homogeneous charge compression ignition engine with variable compression ratio”. SAE paper 1999-01-3679. 1999.

[8] Yao M, Zheng Z, Liu H. “Progress and recent trends in homogeneous charge compression ignition (HCCI) engines”. Prog Energy Combust Sci. 2009. Vol. 35: 398–437.

[9] Bahng GW, Jangb D, Kimc Y, Shin M. “A new technology to overcome the limits of HCCI engine through fuel modification”. Applied Thermal Engineering. 2016. Vol. 98: 810-815.

[10] Chunhua Z, Han W. “Combustion characteristics and performance of a methanol fuelled homogenous charge compression ignition (HCCI) engine”. Journal of the Energy Institute. 2016. Vol. 89: 346-353.]

[11] Dec JE. “A computational study of the effects of low fuel loading”. SAE paper 2002;01-1309. 2002.

[12] Dec JE. “Advanced compression-ignition engines- understanding of the in-cylinder processes”. Proceeding of the Combustion Institute. 2009. Vol. 32: 2727-2742.

[13] Bendu H, Murugan S. “Homogeneous charge compression ignition (HCCI) combustion: mixture preparation and control strategies in diesel engines”. Renewable and Sustainable Energy Reviews. 2014. Vol. 38: 732-746.

[14] Qiang Z, Na L, Menghan L. “Combustion and emission characteristics of an electronically-controlled common-rail dual-fuel engine”. Journal of the Energy Institute. 2016. Vol. 89: 766-781.

[15] Bidarvatan M, Thakkar V, Shahbakhti M, Bahri B, Aziz AA. “Grey-box modeling of HCCI engines”. Applied Thermal Engineering. 2014. Vol. 70: 397-409.

[16] Jiménez-Espadafor FJ, Torres M, Vélez JA, Carvajal E, Becerra JA. “Experimental analysis of low temperature combustion mode with diesel and biodiesel fuels: A method for reducing NOx and soot emissions”. Fuel Processing Technology. 2012. Vol. 103: 57-63.

[17] Jiménez FJ, Torres M, Correa JA, Becerra JA. “Effect of turbulence and external exhaust gas recirculation on HCCI combustion mode and exhaust emissions”. Energy & Fuels. 2009. Vol. 23 (9): 4295–4303.

[18] Vélez Godiño JA, Torres García M, Jiménez-Espadafor Aguilar FJ, Carvajal Trujillo E. “Numerical study of HCCI combustion fueled with diesel oil using a multi-zone model approach.”. Energy Conversion and Management. 2015. Vol. 89: 885–895.

[19] MATLAB 7.8. The MathWorks Inc. 2009.

[20] Aceves SM, Westbrook C, Smith J et al. "A multi-zone model for prediction of HCCI combustion and emissions," SAE Technical Paper 2000-01-0327. 2000.

[21] Heywood JB. “Internal Combustion Engine Fundamentals”. London. McGraw-Hill. 1988.

[22] Bowman CT. “Kinetics of pollutant formation and destruction in combustion”. Prog. Energy Combust. Sci. 1975. Vol 1: 33-45.

[23] Lavole GA, Heywood JB, Keck JC. “Experimental and theoretical investigation of nitric oxide formation in internal combustion engines”. Combust. Sci. Technol. 1970. Vol 1: 313-326.

[24] Megel M, Westmoreland B, Jones G, Phillips F et al. "Development of a Structurally Optimized Heavy Duty Diesel Cylinder Head Design Capable of 250 Bar Peak Cylinder Pressure Operation". SAE Int. J. Engines. 2011. Vol. 4 (3): 2736-2755.

[25] Nishi M, Kanehara M,Iida N. “Assessment for innovative combustion on HCCI engine by controlling EGR ratio and engine speed”. Applied Thermal Engineering. 2016. Vol. 99: 42-60.

[26] Zhao H. (ed). “HCCI and CAI engines for the automotive industry”. Woodhead Publishing. Cambridge. 2007.

[27] Çınar C, Uyumaz A, Polat S, Yılmaz E, Can Ö, Solmaz H. “Combustion and performance characteristics of an HCCI engine utilizing trapped residual gas via reduced valve lift”. Applied Thermal Engineering. 2016. Vol. 100: 586-594.